

## High Efficiency Solar Cooling Technique

Al. Al-Alili<sup>1</sup>, Y. Hwang<sup>1</sup>, R. Radermacher<sup>1</sup>, I. Kubo<sup>2</sup> and P. Rodgers<sup>2</sup>

<sup>1</sup>Department of Mechanical Engineering, University of Maryland, College Park, U.S.A.

<sup>2</sup>Department of Mechanical Engineering, The Petroleum Institute, Abu Dhabi, U.A.E.  
*yhhwang@umd.edu*

### Abstract

A novel application for a hybrid photovoltaic/thermal (PVT) collector, which produces electricity and hot water simultaneously, is investigated. PVT collectors have been used mainly for low temperature application such as domestic hot water production. In this study, the hybrid collector is used to drive a hybrid cooling system. Since latent loads represent a significant portion of the air conditioning loads in hot and humid climates, the hybrid cooling system consists of a solid desiccant wheel cycle (DWC) and a traditional vapor compression cycle (VCC). The DWC is driven by the collector thermal output and the VCC is driven by the electrical output. The system performance was modeled using *Transient Systems Simulation* program and Abu Dhabi weather conditions. A parametric study was carried out to help finalize the complete system size. The system performance was also compared to the performance of the standalone VCC which is widely used in the UAE. The decoupling of the latent and sensible load is found to be very effective in meeting the humidity and temperature requirements of buildings. In addition, this combination increases the cooling COP of the VCC compared to the standalone VCC. Therefore, to provide the same cooling capacity, the proposed system reduces the electrical energy required to drive the VCC by 50%.

### 1. Introduction

In hot and humid regions of the world, removal of moisture from the air represents a major portion of the air conditioning load. Conventionally, air conditioning systems have to lower the air temperature below its dew point for the dehumidification. Then the air has to be heated in order to reach the comfort level. Following this traditional process consumes extra energy and increases peak electricity demands.

Desiccants cycles offer the solution to meet the humidity and temperature requirements of buildings via decoupling latent and sensible loads. Integrating a solid desiccant system with vapor compression air conditioner allows the latter to operate at higher evaporator temperature and pressure. Operating at higher evaporator pressure decreases the cycle pressure ratio, hence increasing the compressor efficiency.

A photovoltaic/thermal (PVT) collector is a combination of photovoltaic (PV) cells with a solar thermal collector which converts solar irradiance into electricity and heat simultaneously. The temperature of the PV cells is increased by the absorbed solar radiation that is not converted into electricity, causing a decrease in their efficiencies. Even the most efficient PV cell today has less than 50% efficiency, which means that more than half the incident solar energy is converted to heat. This motivates the utilization of the generated heat from cooling the PV cells either passively or actively. The cooling media could be liquid (mostly water), air or both. In addition, by combining the two collection technologies in one collector, the amount of energy converted per unit surface area is greater than that of a side-by-side PV panel and thermal collector.

A significant amount of research on PVT collectors has been carried out since middle seventies. The performance of flat PVTs has been investigated theoretically and experimentally. Recently, many theoretical, analytical and numerical, studies have been performed [24, 25, 26, 27, 28]. The electrical and thermal performance of the flat PVT has been also investigated experimentally by various researchers [29, 30, 31]. The thermal output of the PVT has been mainly utilized for domestic hot water applications [24, 25, 29, 32, 33, 34] or direct floor heating [35]. An investigation using Transient Systems Simulation (TRNSYS) [9] has been conducted to study the industrial application of two experimentally tested PVT systems using a-Si and pc-Si. It has been found that in order to keep the electrical and thermal efficiency of PVT systems at an acceptable level, they should be used for applications that need heat in medium temperature level (60-80°C) [37].

The concentrating PVT (CPVT) has not received as much attention as the flat types with regards to modeling, testing and searching for new applications. Brogren *et al.* studied the optical performance of a CPVT using low concentrating Compound Parabolic Concentrator (CPC) having concentration ratio  $C = 4$ , with mono-crystalline silicon cells [38]. Different reflectors had been tried: glass/Ag, TiO<sub>2</sub>/SiO<sub>2</sub>/Al and Al<sub>2</sub>O<sub>3</sub>/Al. It has been concluded that the electric output could be increased by 20% by using optimized antireflection coating and reflectors for high latitude. Moreover, Nilsson *et al.* investigated the electrical

and thermal characteristics of an asymmetric CPC with mono-crystalline silicon cells built for high latitudes [39]. Their collector consisted of two asymmetric concentrators, a front reflector and a back reflector. However, they concluded that the optimal placement of the PV cells was facing the front reflector, which collected most of the irradiation in the summer. Assoa *et al.* studied a new concept where air and water are used to cool a CPC with polycrystalline silicon cells [40]. They developed a two dimensional steady state model of the collector. They investigated the performance of the collector numerically and experimentally to find the effect of various parameters. The performance of a single axis tracking system using a parabolic trough,  $C = 37$ , with mono-crystalline silicon cells was experimentally investigated by Coventry [41]. He studied the impact of the illumination and temperature non-uniformities across the PV cells on the overall electrical performance of the collector. He found that the electrical performance is significantly affected by the shape error, receiver support post shading and gaps between the mirrors. Moreover, a miniature dish concentrator of concentration ratio up to 400 with triple-junction PV cells was theoretically investigated by Kribus *et al.* [42]. They analyzed the electrical and thermal performance as well as the manufacturing cost and the resulting cost of energy in the case of domestic water heating. Later, Mittelman *et al.* coupled the miniature dish collector with LiBr/H<sub>2</sub>O absorption cycle, operating at rejection temperature of 25°C and evaporator temperature of 10°C [43].

From the literature review, it was found that not only there is a limitation on the literature available on CPVT, but also their applications. There have been a few attempts to utilize the thermal output in other applications besides domestic water heating. The novelty of this study is to use a CPVT collector to drive a thermally and an electrically driven cycles for air conditioning application, simultaneously. A desiccant wheel cycle (DWC), which is driven by the thermal output of the collector, is used to accommodate the latent load. A vapor compression cycle (VCC), which is powered by the electric output of the collector, is used to accommodate the sensible load. This design is expected to use minimal external energy and it is believed to lead to the highest overall system Coefficient of Performance (COP) to date.

## 2. System Description

The system is divided into two main sub-systems: solar sub-system and cooling sub-system. The solar sub-system consists of the solar collector, a thermal storage, an electrical storage, a regulator, an inverter and controllers. The solar sub-system can be seen in Figure 12. As the figure shows, storage for each type of the energy output of the collector is used. The main purpose of these storages is to serve as a buffer reservoir to provide nearly constant outputs.

The cooling sub-system includes the two cooling processes, VCC and DWC, the conditioned space and the required fans and controllers, as shown in Figure 13. The conditioned space in this study represents a residential home to be conditioned. As indicated in the figure, the thermal output of the solar sub-system is used to regenerate the desiccant wheel by heating the building exhaust air stream in the water-air heat exchanger. Moreover, the electrical output of the solar sub-system is used to drive the VCC. The figure also shows that part of the air leaving the building is sent to the DWC, through a heat recovery wheel (HRW), to be exhausted and the remaining air is re-circulated. The HRW is used to sensibly cool the hot and dehumidify air leaving the DWC before being mixed with the re-circulating air. The amount of air exhausted is replaced by fresh air which is pretreated in the DWC and then mixed with the re-circulating

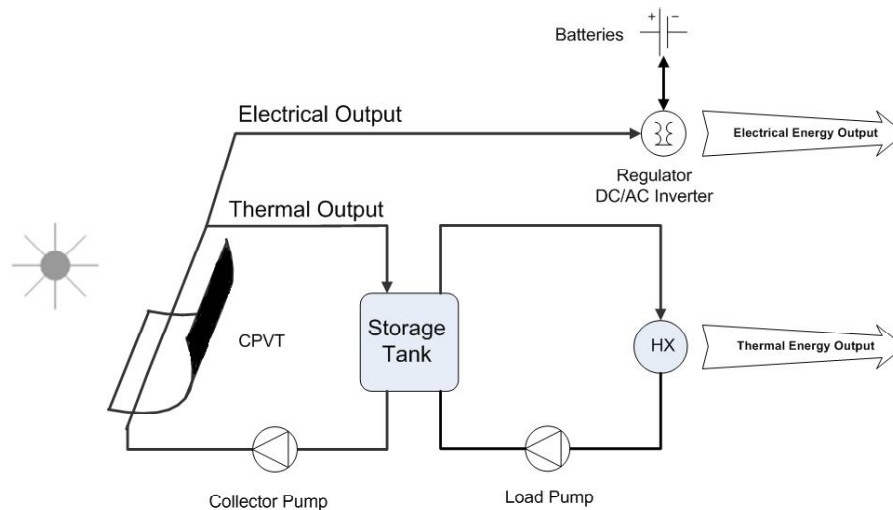


Figure 12. The solar sub-system.

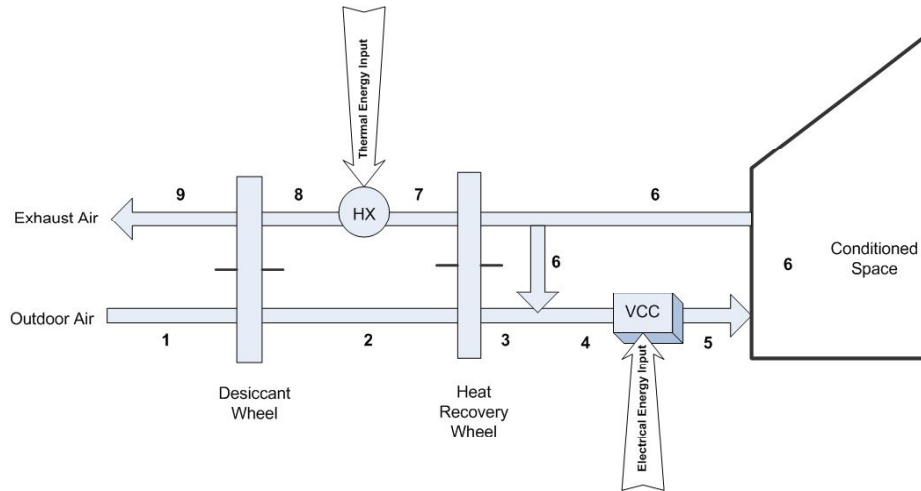


Figure 13. The cooling sub-system.

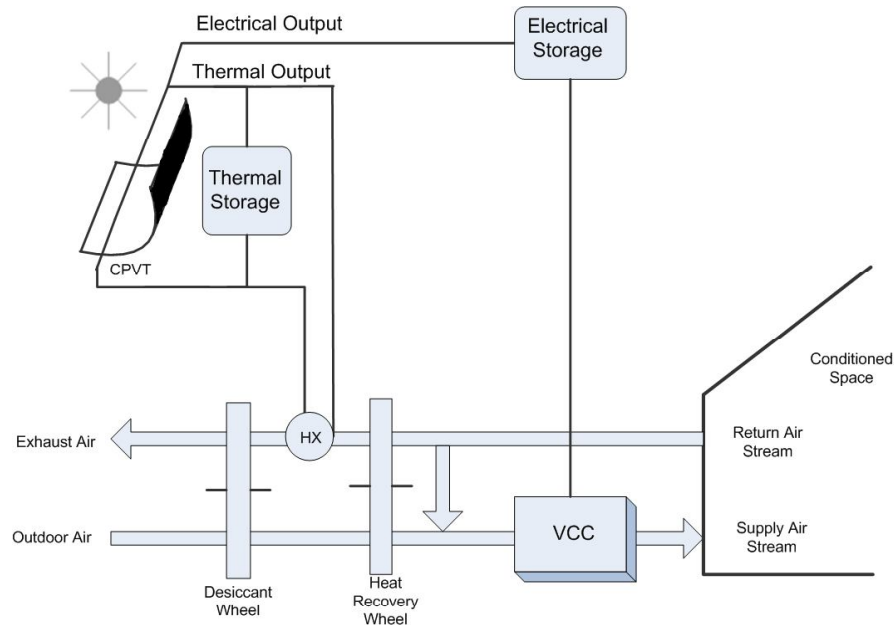


Figure 14. Schematic of the solar cooling system.

air stream before being sent to the VCC. The cooling sub-system can be possible coupled with the solar sub-system to construct the complete system as shown in Figure 14.

### 3. System Modeling

The modeling approach is shown in Figure 15. By calculating the supplied electrical and thermal energy from the solar sub-system and the required heat and power by the cooling processes, the solar fraction of each type of energy provided can be calculated. A thermal solar fraction (TSF) and an electrical solar fraction (ESF) can be calculated as shown in Equations (3) and (4), respectively.

$$TSF = \frac{Q_{provided}}{Q_{required}} \quad (3)$$

$$ESF = \frac{P_{provided}}{P_{required}} \quad (4)$$

The system is modeled with TRNSYS program [9]. TRNSYS consists of many subroutines, called Types, which model subsystem components. In each model, the relationships between the input and output are defined. Then, the models are linked together to form a system model. TRNSYS solves the set of equations created by the system at each time step. The user has to define the components' parameters and decide on the information transferred from one component to the other. Therefore, it is necessary to construct an information flow diagram for the system once all the components of the system have been identified. The information flow diagram for the whole system is created as shown in Figure 16. The main purpose of this diagram is to facilitate identification of the various components and the flow of information between them.

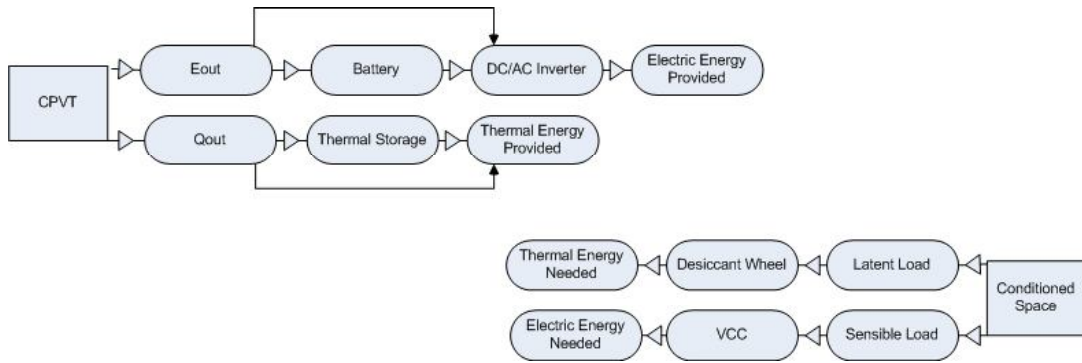


Figure 15. Modeling approach.

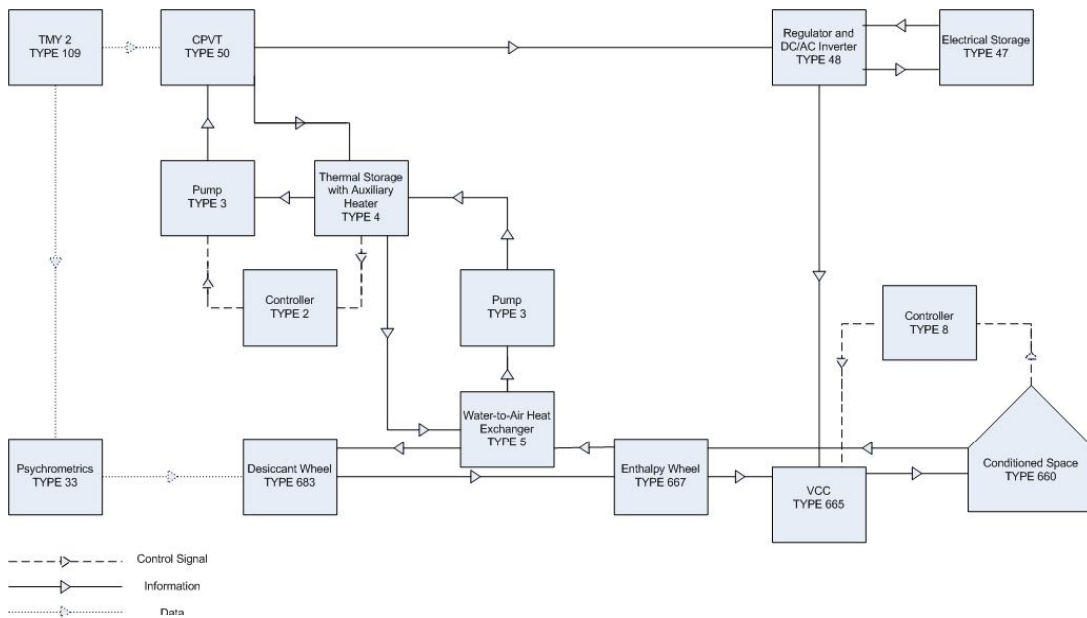


Figure 16. System information flow diagram.

The collector array is sized to deliver  $8 \text{ kW}_e$  and the  $34 \text{ kW}_{th}$  at  $800 \text{ W/m}^2$  and  $25^\circ\text{C}$  weather conditions. In order to achieve this output, two rows of five collectors connected in series are used. Two different efficiencies can be defined for the CPVT collector namely, electrical and thermal efficiencies. The electrical and thermal efficiencies ( $\eta_{elec}$ ,  $\eta_{th}$ ) can be calculated based on Equations (5) and (6), respectively.

$$\eta_{elec} = \frac{P_{coll_{out}}}{G_d A_a} \quad (5)$$

$$\eta_{th} = \frac{Q_{coll_{out}}}{G_d A_a} \quad (6)$$

Moreover, the VCC is modeled based on a commercially available 17.5 kW unit using R410A [44]. The unit chosen is capable of providing heating and cooling during the winter and summer, respectively. The manufacturer's data are arranged in a format that TRNSYS can recognize. The VCC is sized to provide 15 kW of cooling at ASHRAE 1% design conditions for Abu Dhabi shown in Table 6. The COP of the VCC ( $COP_{VCC}$ ) can be defined as shown in Equation

(7):

$$COP_{VCC} = \frac{Q_{evap}}{P_{comp}} \tag{7}$$

In addition, the DWC is sized to deliver 5 kW at ASHRAE 1% design conditions for Abu Dhabi and an air mass flow rate of 700 kg/hr, as shown in Table 6.

The COP of a desiccant cooling system ( $COP_{DWC}$ ) is defined as the ratio between the enthalpy change from ambient air to supply air, multiplied by the mass flow rate and the heat delivered to the water-air heat exchanger (HX), as given by Equation (8):

$$COP_{DWC} = \frac{m^*(h_{amb} - h_{sup})}{Q^*_{reg}} \tag{8}$$

The performance of the cooling sub-system is investigated prior to constructing the complete system. The cooling sub-system is tested at  $T_{amb} = 45^\circ\text{C}$  and  $w_{amb} = 15 \text{ g}_w/\text{kg}_a$ , and the temperature and humidity ratio at various points are recorded. Figure 17 shows the psychrometric processes indicated in Figure 13.

Once the sub-systems are joined to form the complete solar cooling system, the whole system COP can be defined as shown in Equation (9):

$$COP_{sys} = COP_{elec} + COP_{th} \tag{9}$$

where the  $COP_{elec}$  is the electrical efficiency of the CPVT multiplied by the  $COP_{VCC}$  and the  $COP_{th}$  is the thermal efficiency of the CPVT multiplied by the  $COP_{DWC}$ .

Table 6. ASHRAE design conditions for Abu Dhabi [45].

	Air Conditioning (1%)		Desiccant Cooling (1%)
DB	42.5°C	DP	28.8°C
MWB	23.4°C	W	0.025 kg <sub>w</sub> /kg <sub>a</sub>
		MDB	32.8°C

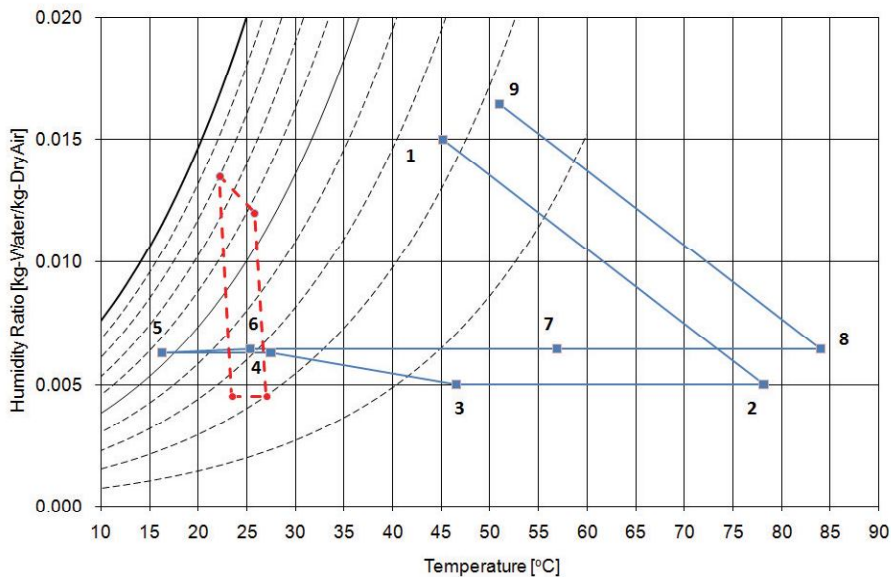


Figure 17. Air state points in various locations in the cooling sub-system.

A brief description of the other components used in TRNSYS simulation of the whole system can be found in Table 7.

#### 4. Parametric Study

A Typical Meteorological Year 2, *TMY2*, data file is used to obtain the solar irradiance and various weather conditions for Abu Dhabi [46]. The initial configuration of the solar sub-system consists of a 1 m<sup>3</sup> hot water storage tank and 12 batteries. The initial operation conditions are a water mass flow rate (MFR) through the collectors array of 1,800 kg/hr and water MFR through the water-air heat exchange of 1,500 kg/hr.

The water MFR through the collector array is varied to investigate its effect on the thermal and electrical outputs. It has to be noted that, in PVT system applications, the production of electricity is the main priority. Figure 18 shows that as the water MFR through the collector array increases the thermal

**Table 7: Parameters of various key components used in TRNSYS simulation**

Component	Parameter	Value
Simple lumped capacitance multi-zone building model	UA	1,000 kJ/hr.K
	Capacitance of zone	24,000 kJ/K
Thermal storage tank	Volume	250 m <sup>3</sup>
	T <sub>init</sub>	30°C
	W <sub>init</sub>	0.013 kg <sub>w</sub> /kg <sub>a</sub>
	Infiltration flow rate	75 kg/hr
	Tank volume	1 m <sup>3</sup>
Thermal storage tank	Water specific heat	4.19 kJ/ kg.K
	Water density	1,000 kg/m <sup>3</sup>
	Tank loss coefficient	3 kJ/hr.m <sup>2</sup> .K
	Number of nodes	10
	Height of each node	0.05 m
	Boiling point	100°C
Regulator and inverter DC/AC	Regulator efficiency	0.78
	Inverter efficiency	0.96
	High limit on fractional state of charge	0.25
	Inverter output power capacity	54,000 kJ/kg
Electrical storage	Cell energy capacity	125 AH
	Cells in parallel	12
	Cells in series	6
	Charging efficiency	0.9
	Max. current per cell charging	3.33 A
	Max. current per cell discharge	-3.33 A
	Max. charge voltage per cell	2.5 V
VCC	Total air flow rate	2,973 m <sup>3</sup> /hr
	Rated indoor fan power	671 kJ/hr
	Rated outdoor fan power	745 kJ/hr
Desiccant wheel	Dehumidifier F1 effectiveness	0.08
	Dehumidifier F2 effectiveness	0.95
Heat recovery wheel	Rated power	671 kJ/hr
	Sensible effectiveness	0.75
	Latent effectiveness	0

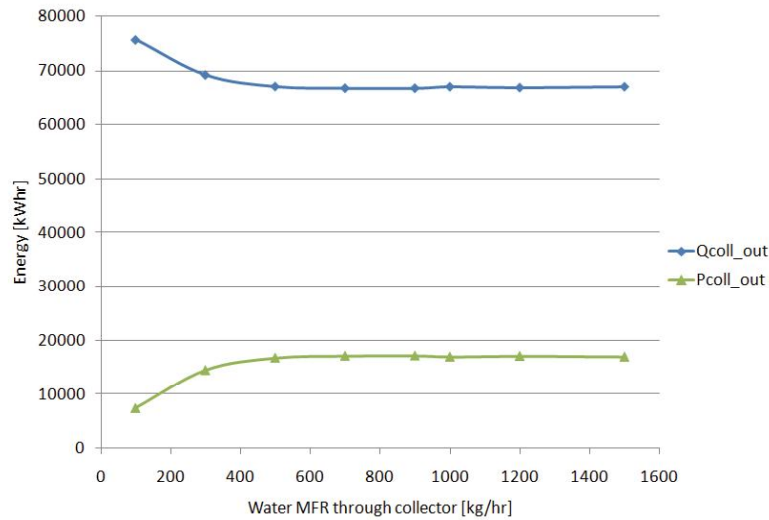


Figure 18. The effect of the collector MFR on its outputs.

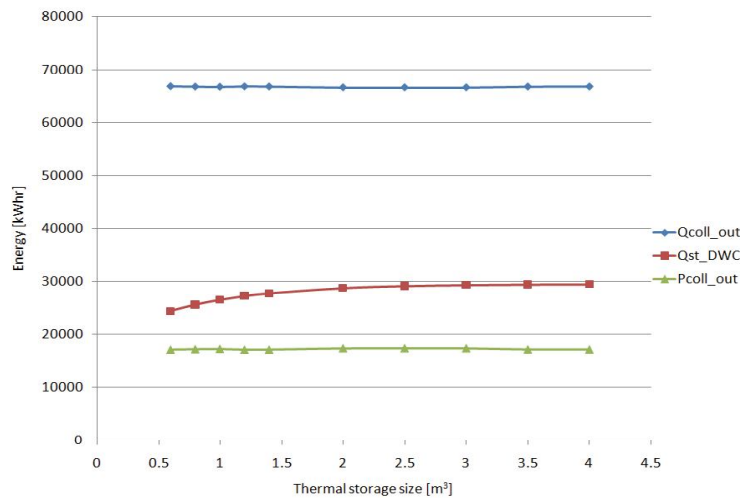


Figure 19. Thermal storage size vs. energy delivered.

output decreases until it reaches a nearly constant value. On the other hand, the electrical output increases until it becomes flat. As the water MFR increases, the increase in the water temperature decreases, which leads to lower PV cells temperature. The lower the PV cell temperature, the higher the efficiency, hence the electricity production.

The volume of the hot water storage tank is varied to investigate its effect on the collector outputs and the amount of energy delivered to the DWC through the water-air HX. As indicated by Figure 19, the collector electrical and thermal outputs are steady. However, the amount of energy delivered to the DWC increases with increasing thermal storage size. It should be noted that increasing the thermal storage volume beyond 2 m<sup>3</sup> does not have significant effects on the energy delivered to the DWC.

Two power conditioning devices are used for the collector's electrical output. The first one is a regulator, which distributes DC power from the collector array to/from the battery array. The second device is the inverter which converts the DC power to AC and sends it to the VCC. These two components are represented by a TRNSYS TYPE 48 as shown in Figure 16. Based on the VCC required energy, TYPE 48 will decide on whether to use the collector output or the grid. The priority is given to utilizing the electrical output of the collector directly to drive the VCC and the surplus is directed to charging the batteries. Figure 20 shows the effect of increasing the electrical storage size on the electrical energy delivered by the grid. As the number of batteries increases the needed grid energy decreases.

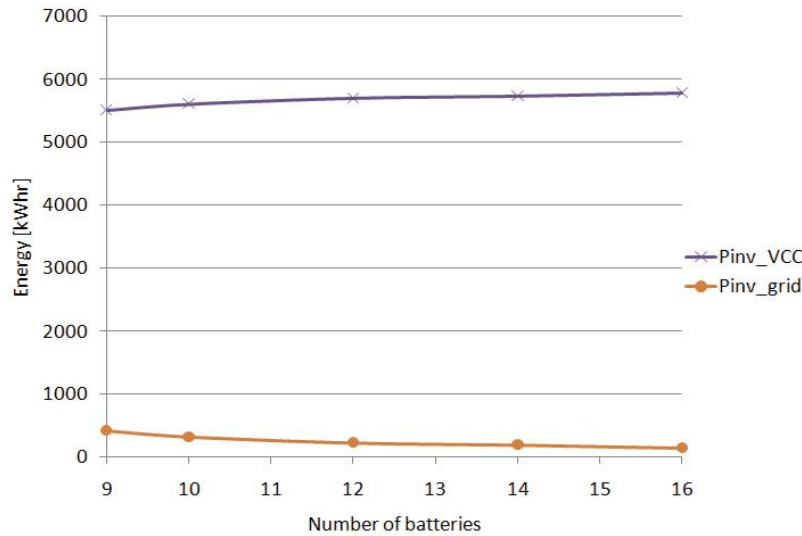


Figure 20. Effect of the electrical storage size on the electrical energy delivered.

### 5. Overall System Behavior

Finally, the whole system is constructed by coupling the two sub-systems and the monthly performance is investigated. The main parameters used for simulating the complete system can be found in Table 8. The hourly space temperature for a complete year is plotted in the psychrometric chart as shown in Figure 21 to ensure that it is in the comfort zone during the simulation. It has to be noted that about 10% of the mass flow rate of the air leaving the conditioned space is sent to the DWC and the rest is re-circulated to be mixed with the preconditioned air in the DWC as indicated by Figure 14.

Figure 21 shows how effective the combination of the DWC and VCC is in obtaining the comfort level inside buildings located in hot and humid locations. It can be seen that the hourly conditions inside the building range from a temperature of 20°C to 25°C and a humidity ratio of about 0.005 to 0.008 kg<sub>w</sub>/ kg<sub>a</sub>. The performance of the system is compared to the performance of a VCC alone. The hourly space temperature for one year simulation for the case of VCC alone, without a DWC, can be seen in Figure 22. It can be seen that the VCC alone is not as effective as the proposed system in keeping the space conditions inside the comfort zone.

The advantage of the pretreatment of the air by the DWC before entering the VCC can be seen very clearly in Figure 23, which shows the sensible and the latent load on the VCC when the DWC is ON. It indicates that when the DWC accommodates the latent load, the VCC has to accommodate the sensible load only. By treating latent and sensible loads separately, the VCC can be operated at higher evaporating pressure hence reducing the cycle pressure ratio and increasing the compressor efficiency. The latent load that is shown is due to the re-circulating of the space air which includes moisture from the internal latent load sources and infiltration.

Figure 24 shows the case when the DWC is turned OFF. In this case, the VCC has to accommodate the extra latent load introduced by ventilation in addition to the space latent load. This requires decreasing the evaporator's temperature below the dew point of the incoming air in order to condense the moisture. It can be seen that the latent load is higher during summer since the air temperature is higher; hence its capability of holding more moisture increases.

Table 8. Main specifications of the completed cooling system.

Component	Parameter	Value
CPVT	Mass flow rate	700 kg/hr
Thermal storage tank	Volume	2 m <sup>3</sup>
Water-air heat exchanger	Water mass flow rate	500 kg/hr
Electrical storage	Number of batteries	12

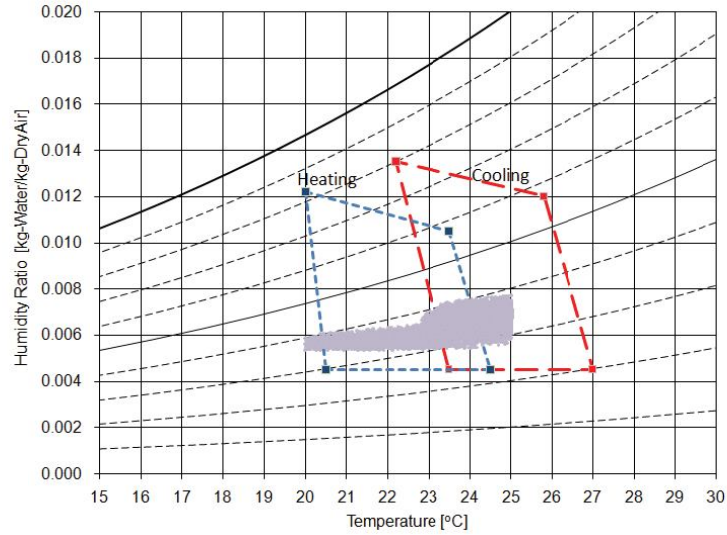


Figure 21. The hourly space conditions for one year simulation.

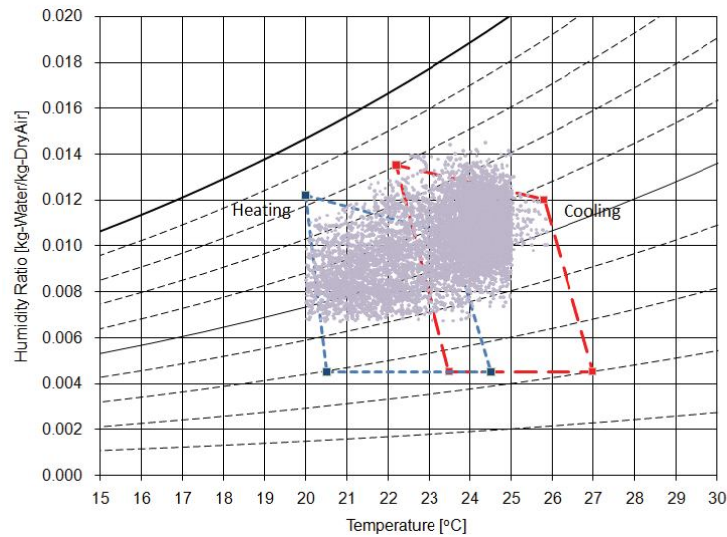


Figure 22. The hourly space conditions for VCC only.

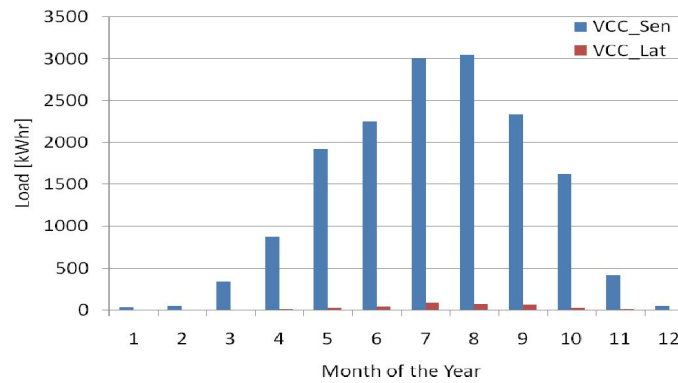


Figure 23. Monthly sensible and latent loads on the VCC (VCC + DWC).

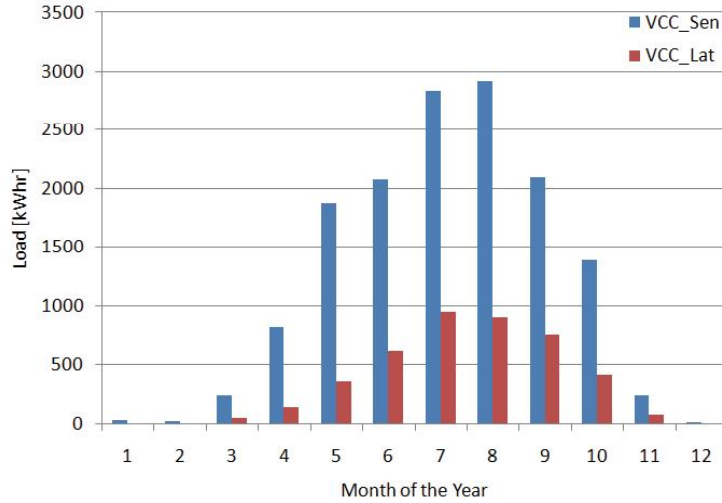


Figure 24. Monthly sensible and latent loads on the VCC (VCC only).

The monthly CPVT electrical and thermal efficiencies and the cooling cycles' COPs are shown in Table 9. The heating season is considered to be from December to February, whereas the cooling season is from March to November. It can be seen that the overall system COP is above unity. The current solar thermally driven cycles have low COPs due to the limitation on the thermally driven cooling cycles. In addition, the solar electrically driven cycles have low COPs due to the low electrical conversion efficiency of the PV cells. However, the proposed system eliminates these penalties by keeping the CPVT at high electrical conversion efficiency by the forced convective cooling of the PV cells. In addition, separating the latent and the sensible load contributes in increasing the COPs of the cooling cycles further. Moreover, the average COP<sub>VCC</sub> during the cooling season was found to be 3.92 compared to the standalone VCC's COP of 2.51. The COP<sub>elec</sub> of the hybrid system can be compared to the COP<sub>elec</sub> of the standalone VCC powered by PV panels. The efficiency of the PV cells is expected to be lower than that of the actively cooled PV cells, since the efficiency decreases as the temperature increases. Therefore, if a 12% efficient PV cells used to power the standalone VCC, the COP<sub>elec</sub> would be 0.3 compared to the proposed system's average COP<sub>elec</sub> of 0.62.

Table 9. Final system monthly performance.

Month	$\eta_{elec}$	$\eta_{th}$	COP <sub>VCC</sub>	COP <sub>DWC</sub>	COP <sub>elec</sub>	COP <sub>th</sub>	COP <sub>sys</sub>
1	0.17	0.64	4.73	0.95	0.78	0.61	1.39
2	0.17	0.64	4.41	1.04	0.73	0.66	1.39
3	0.17	0.64	3.48	1.24	0.58	0.79	1.37
4	0.16	0.64	3.97	1.37	0.64	0.88	1.51
5	0.16	0.64	3.97	1.46	0.65	0.93	1.58
6	0.16	0.64	3.97	1.43	0.64	0.91	1.55
7	0.16	0.64	3.98	1.46	0.64	0.93	1.57
8	0.16	0.64	3.98	1.47	0.65	0.93	1.59
9	0.17	0.64	3.98	1.43	0.66	0.91	1.57
10	0.17	0.63	3.97	1.38	0.68	0.87	1.55
11	0.17	0.63	3.97	1.26	0.68	0.79	1.47
12	0.17	0.63	3.43	1.17	0.57	0.74	1.31

## 6. Conclusions

There is a scarcity on the concentrating photovoltaic/thermal (CPVT) collector modeling and applications in the literature. It has been found that the utilization of the thermal output of these hybrid collectors is limited to domestic hot water production. A novel solar cooling system which consists of a hybrid cooling system and a hybrid collector was investigated. TRNSYS simulation program was used to model the system performance. The cooling cycle performance was sized based on ASHRAE design conditions for Abu Dhabi. A parametric study was carried out to study the sensitivity of the system performance to mass flow rate through the collector array, thermal storage size and electrical storage size. Integrating a DWC with a conventional VCC is found to ensure comfort of a conditioned space more effectively than the standalone VCC. In addition, this combination increases the cooling COP of the VCC compared to the standalone VCC. Therefore, to provide the same cooling capacity, the proposed system reduces the electrical energy required to drive the VCC by 50%.

## Nomenclature

<b>Abbreviation</b>	<b>Description</b>	<b>Unit</b>
C	Concentration Ratio	-
COP	Coefficient of Performance	-
CPC	Compound Parabolic Collector	-
CPVT	Concentrating Photovoltaic/Thermal	-
DB	Dry Bulb temperature	°C
DP	Dew Point temperature	°C
DWC	Desiccant Wheel Cycle	-
ESF	Electrical Solar Fraction	-
HRW	Heat Recovery Wheel	-
HX	Heat Exchanger	-
MDB	Mean coincident Dry Bulb temperature	°C
MFR	Mass Flow Rate	kg/hr
MWB	Mean coincident Wet Bulb temperature	°C
TMY2	Typical Meteorological Year 2	-
TRNSYS	Transient Systems Simulation	-
TSF	Thermal Solar Fraction	-
PV	Photovoltaic	-
PVT	Photovoltaic/Thermal collector	-
UAE	United Arab Emirates	-
VCC	Vapor Compression Cycle	-
W	Humidity Ratio	kg <sub>w</sub> /kg <sub>a</sub>
<b>Symbol</b>	<b>Description</b>	<b>Unit</b>
T	Temperature	°C
Q*	Thermal capacity	kJ/hr
P	Electrical power	kJ/hr
m*	Mass flow rate	kg/hr
h	Enthalpy	kJ/kg
G	Solar irradiance	kJ/hr-m <sup>2</sup>
η	Efficiency	-
A	Area	m <sup>2</sup>
<b>Subscript</b>		
d	Direct component of the solar irradiance	-
a	Aperture	-
reg	Regeneration	-
comp	Compressor	-
sup	Supply to the mixer before the VCC	-
coll_out	Collector energy output	-
lat	Latent	-
sen	Sensible	-
amb	Ambient	-
elec	Electrical	-
th	Thermal	-
st_DWC	Thermal storage tank to the DWC	-
inv_VCC	Inverter to VCC	-
inv_grid	From the grid to the inverter	-
sys	System	-

## References

24. Zondag, H.A., De Vries, D.W., Van Helden, W.G.J., Van Zolingen, R.J.C. and Van Steenhoven, A.A., "The thermal and electrical yield of a PV-Thermal collector," *Solar Energy*, Vol. 72, (2002), pp. 113–128.
25. Chow, T.T., "Performance analysis of photovoltaic-thermal collector by explicit dynamic model," *Solar Energy* Vol. 75, (2003), pp. 143–152.
26. Lazarova, V., Schaeffer, Chr., Shishkova, M. and Lvanovab, M., "Hybrid solar collector," *Journal of material processing technology*, Vol. 161, (2005), pp. 229-233.
27. Vokas, G., Christandonis, N. and Skittides, F., "Hybrid photovoltaic-thermal systems for domestic heating and cooling - A theoretical approach," *Solar Energy*, Vol. 80, (2006), pp. 607–615.
28. Santbergen, R. and van Zolingen, R.J., "Modeling the thermal absorption factor of photovoltaic/thermal combi-panels," *Energy Conversion and Management*, Vol. 47, (2006), pp. 3572–3581.
29. Fujisawa, T. and Tani, T., "Optimum Design for Residential photovoltaic- Thermal Binary Utilization System by Minimizing Auxiliary Energy," *Electrical Engineering in Japan*, Vol. 137, (2001), pp. 28-35.
30. Sandnes, B. and Rekstad, J., "A Photovoltaic/Thermal (Pv/T) Collector with a Polymer Absorber Plate. Experimental Study and Analytical Model," *Solar Energy*, Vol. 72, (2002), pp. 63–73.
31. Robles-Ocampo, B., Ru, E., Vasquez, Z., Canseco, H., Nchez, Sa., Cornejo-Meza, R.C., Tra'paga-Martí'nez, G., Garcí'a-Rodríguez, F.J., Gonza'lez-Herna'ndez, J. and Vorobiev, Yu.V., "Photovoltaic/thermal solar hybrid system with bifacial PV module and transparent plane collector," *Solar Energy Materials & Solar Cells*, Vol. 91, (2007), pp. 1966-1971.
32. Zondag, H.A., De Vries, D.W., Van Helden, W.G.J., Van Zolingen, R.J.C. and Van Steenhoven, A.A., "The yield of different combined PV-thermal collector designs," *Solar Energy*, Vol. 74, (2003), pp. 253–269.
33. Tiwari, A. and Sodha, M.S., "Performance evaluation of solar PV/T system: An experimental validation," *Solar Energy*, Vol. 80, (2006), pp. 751–759.
34. Kalogirou, S.A. and Tripanagnostopoulos, Y., "Hybrid PV/T solar systems for domestic hot water and electricity production," *Energy Conversion and Management*, Vol. 47, (2006), pp 3368–3382.
35. Fraisse, G., Me'ne'zo, C. and Johannes, K., "Energy performance of water hybrid PV/T collectors applied to combisystems of Direct Solar Floor type," *Solar Energy*, Vol.81, (2007), pp. 1426–1438.
36. TRNSYS, "A Transient Simulation Program," Vers. 16.1, Solar Energy Laboratory, University of Wisconsin, Madison, (2006).
37. Kalogirou, S.A. and Tripanagnostopoulos, Y., "Industrial application of PV/T solar energy systems," *Applied Thermal Engineering*, Vol. 27, (2007), pp. 1259-1270.
38. Brogren, M., Nostell, P. And Karlsson, B., "Optical Efficiency of a PV–Thermal Hybrid CPC Module For High Latitudes," *Solar Energy*, Vol. 69, (2000), pp. 173–185.
39. Nilsson, J., Hakansson, H. and Karlsson, B., "Electrical and thermal characterization of a PV-CPC hybrid," *Solar Energy*, Vol. 81, (2007), pp. 917–928.
40. Assoa, Y.B., Menezes, C., Fraisse, G., Yezou, R. and Brau, J., "Study of a new concept of photovoltaic-thermal hybrid collector," *Solar Energy*, Vol. 81, (2007), pp. 1132–1143.
41. Coventry, J. "Performance of a concentrating photovoltaic/thermal solar collector," *Solar Energy*, Vol. 78, (2005), pp. 211-222.
42. Kribus, A., Kaftori, D., Mittelman, G., Hirshfeld, A., Flitsanov, Y. and Dayan, A., "A miniature concentrating photovoltaic and thermal system," *Energy Conversion and Management*, Vol. 47, (2006), pp. 3582–3590.
43. Mittelman, G., Kribus, A. and Dayan, A., "Solar cooling with concentrating photovoltaic/thermal (CPVT) systems," *Energy Conversion and Management* Vol. 48, (2007), pp. 2481–2490.
44. Trane, "Product Data: 4DCZ6036A through 4DCZ6060A" (2008), 22-1815-03.
45. ASHRAE. "2001 ASHRAE Fundamentals Handbook: Heating, Ventilating, and Air-Conditioning Applications," American Society of Heating, Refrigeration and Air Conditioning Engineering Inc., (USA, 2001), CH.27.
46. Meteororm, "Global Meteorological Database for Engineers, Planners and Education"(2007).

## Author Biographies

**Mr. Ali Al-Alili** is currently pursuing his Ph.D. degree at the University of Maryland, U.S.A. He worked as a research assistant at the Petroleum Institute (2006-2007) after his graduation from Arizona State University (2006). His research interests are focused on solar powered cooling processes.

**Dr. Yunho Hwang** is a Research Associate Professor in the Department of Mechanical Engineering at the University of Maryland, U.S.A. His research focuses on developing comprehensive information for the detailed physics of transport processes, new cost-effective test methods, and innovative components and systems. He is responsible for the Alternative Cooling Technologies and Applications Consortium (ACTA) that is sponsored by industry, government and research institutions.

**Dr. Reinhard Radermacher** is a Professor in the Department of Mechanical Engineering at the University of Maryland, U.S.A. He holds a M.S. and Ph.D. in Physics from the Munich Institute of Technology. Dr. Radermacher is an internationally recognized expert in heat transfer and working fluids for energy conversion systems, including heat pumps, air-conditioners, and refrigeration systems.

**Dr. Isoroku Kubo** is an Associate Professor at the Petroleum Institute, U.A.E. He is an expert in energy conversion, heat transfer and fluid flow and an internationally recognized authority for his work on solar energy-driven power generation. Dr. Kubo has many years of industrial experience in the areas of diesel engine research and development, solar energy system development as well as management and general product development. In 2001, he joined McNeese State University (MSU) in the U.S. before coming to The Petroleum Institute in December 2004. Dr. Kubo holds a MBA degree from Indiana University, in addition to his Ph.D. in mechanical and aerospace engineering from Cornell University.

**Dr. Peter Rodgers**, Ph.D., is Associate Professor of Mechanical Engineering at The Petroleum Institute, U.A.E. He has extensive experience in thermofluid modeling and experimental characterization. His current research activities are focused on waste heat utilization in the oil and gas industry; the development of polymeric heat exchangers for sea water cooling applications; computational fluid dynamics; electronics reliability; and engineering education. He is presently a member of several international conference program committees, and serves as program co-chair for both EuroSimE 2009 and Energy 2030. He has authored or co-authored over 60 journal and conference publications.